Japanese Journal of Applied Physics
Vol. 46, No. 10A, 2007, pp. 6514–6518

Structural Change and Its Electrooptical Effects on Terahertz Radiation with Post-Growth Annealing of Low-Temperature-Grown GaAs

Doo-Hyeb YOUN, Seong-Jin KIM[1], Gil-Ho KIM[2], and Kwang-Yong KANG

IT Components and Materials Technology Research Division, Electronics and Telecommunications Research Institute, Daejeon 305-350, Korea
[1]*Mitsubishi Cable Industries Ltd., 8 Nishino-cho, Amagasaki, Hyogo 660-0856, Japan*
[2]*School of Information and Communication Engineering and Advanced Institute of Nanotechnology (SAINT), Sungkyunkwan University, Suwon 440-746, Korea*

(Received March 26, 2007; accepted July 24, 2007; published online October 9, 2007)

This paper investigate how post-growth annealing of low-temperature grown GaAs (LT-GaAs) affects, the structural changes induced by the generation of point defects, as well as strain relaxation, the intensity and coarsening of As clusters with annealing, and the carrier recombination lifetime. The intensity and coarsening of As clusters is revealed by the analysis of bright field and high-resolution transmission electron microscopy (HR-TEM). The structural change is determined by the analysis of the intensity as well as a satellite reflection and a peak shift of the X-ray Bragg reflection. The investigation of the defect structures and the carrier lifetime change in the LT-GaAs are based on measurements of HR-TEM, X-ray, Hall, and terahertz spectrum. A systematic study of as-grown and post-growth annealed LT-GaAs reveals that the carrier lifetime is directly related to the intensity and distance of the As clusters. The electrical resistance of the LT-GaAs increases as the annealing temperature increases. A post-growth annealing condition was investigated for emitting and detecting terahertz signals and a photoconductive type dipole antenna was fabricated on the LT-GaAs. [DOI: 10.1143/JJAP.46.6514]

KEYWORDS: LT-GaAs, terahertz, defect, double-crystal X-ray diffractometer, high-resolution transmission electron microscopy, Hall, terahertz spectrum

1. Introduction

Low-temperature grown GaAs (LT-GaAs) has been under investigation for the last 17 years.[1)] The growth of LT-GaAs at 200 °C with an excess of the group V element leads to a nonstoichiometric layer, which significantly alters the electrical[2–5)] and optical[6,7)] characteristics such as carrier lifetime, resistance, and terahertz radiation properties significantly. Moreover, the electrooptical characteristics depend on the post-growth annealing conditions. Due to the unique properties of LT-GaAs, such as the high resistance after annealing and the short carrier recombination time, these layers are used as a high-resistance buffer and insulating cap[1,8)] or in ultrafast photoconductive switches and mixers for terahertz frequencies.[9,10)] Due to a large concentration of point defects, LT-GaAs is conductive while growing but becomes semi-insulating after annealing. During post-growth annealing, the excess As atoms precipitate to from an As cluster. For our investigation, we used high-resolution transmission electron microscopy (HR-TEM) and the X-ray Bragg reflection (X-ray). The HR-TEM is suitable for investigating the structural change in an LT-GaAs layer that results from the formation of As clustering and X-ray is very sensitive to any strain change induced by the configuration of defect.

Emitters and detectors of terahertz both require a short carrier lifetime so that the crystal properties can respond in a subpicosecond (terahertz) time scale. The carrier lifetime of LT-GaAs is known to be as short as 90 fs. However, LT-GaAs has low resistance caused by the hopping conduction between point defects induced by the As incorporation of excess As. An additional problem in LT-GaAs is that the saturation of defect states owing to the charge accumulation. This saturation occurs because the electron–hole recombination time is several orders longer than the trapping time. This saturation effects are overcome by the relatively large density of the states in the precipitates induced by post-growth annealing. Furthermore, the annealing increases the resistance by up to 5 orders of magnitude, and the lifetime often increases often from 500 to 1.6 ps orders. Thus, compromise is important between the carrier lifetime and the resistance with annealing.

We now report on how post-growth annealing affects the structural change that occurs as a result of lattice relaxation, the coarsening and density of As clusters, resistance, and the carrier lifetime of LT-GaAs. In particular, our concerns are concentrated on the use of LT-GaAs to optimize post-growth annealing conditions for obtaining the terahertz emission.

2. Experimental Methods

We grew 1.2-μm-thick undoped LT-GaAs layers by means of molecular beam epitaxy (MBE) on (001) GaAs substrates at a fixed As/Ga beam equivalent pressure ratio of 20. The growth temperature (T_g) was 290 °C. To investigate how the annealing temperature influences changes in the structure and carrier lifetime. LT-GaAs was annealed at temperatures raging from 400 to 600 °C for 10 min by using MBE in an As atmosphere (sample A). The As atmospheric pressure was maintained at 3×10^{-6} Torr during annealing. Because the maximum temperature of the MBE is 600 °C, we used rapid-thermal annealing to perform extra annealing at temperatures higher than 600 °C in an N_2 atmosphere (sample B).

To obtain the structural information, we used a Philips CM20 TEM operated with an acceleration voltage of 200 kV; we also used the Gatan image acquisition system. Cross-sectional specimens were prepared by a face-to-face method. Mechanical polishing and dimpling was then followed by application of the Fischione ultralow-angle ion milling system. Next, we used high resolution double-crystal X-ray diffraction, incorporating a four-bounce monochromator[11,12)] and a standard laboratory X-ray source. X-ray diffraction rocking curves were taken with Cu $K\alpha_1$ radiation and 400 symmetric reflections from GaAs. We investigated the electrical properties by using van der Pauw structures. The Hall measurements yielded resistance values for all the LT-

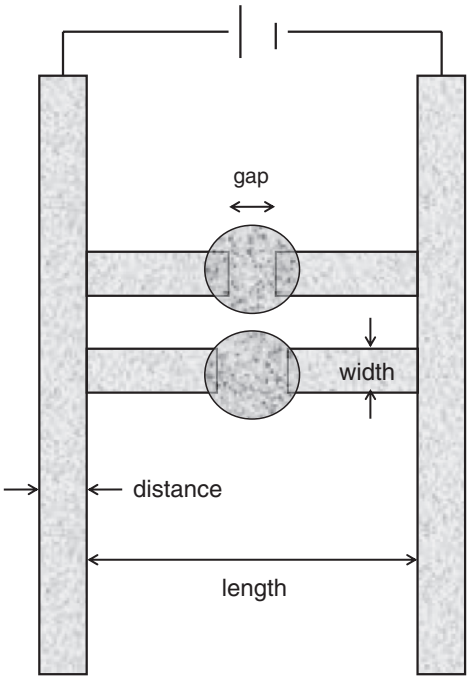

Fig. 1. Schematic view of the photoconductive dipole antenna.

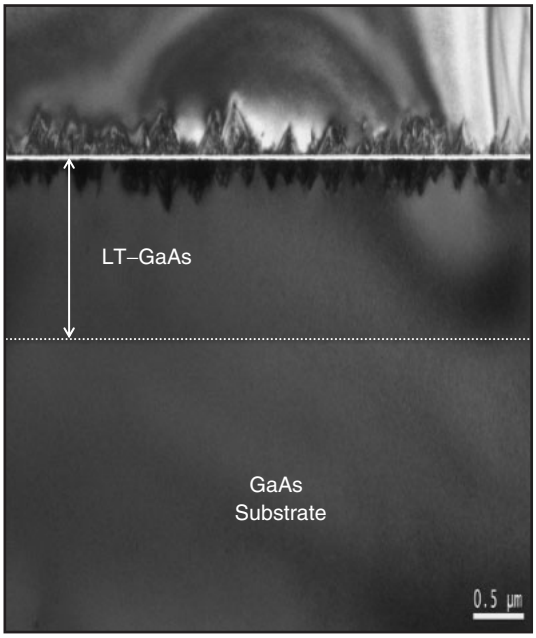

Fig. 2. Cross-sectional view of LT-GaAs samples without annealing.

GaAs samples. Figure 1 shows a schematic view of the photoconductive dipole antennas. The specific dimensions of the antenna structures with small photoconductive gaps of 5 and 10 μm are located at the center of a 10 mm long coplanar transmission line. The photoconductive strip line was a 10 μm wide coplanar line with a separation of 30 μm.

3. Results and Discussion

Figure 2 shows a bright field (BF) TEM cross-sectional image of the as-grown LT-GaAs sample without annealing. A distinct epilayer with a thickness of approximately 1.2 μm is distinguishable from the GaAs substrate; this distinction may be due to a large deviation from the stoichiometry or to the stress that builds up in the LT-GaAs during the low-temperature growth. The as-grown LT-GaAs is highly nonstoichiometric with the excess As manifested in the form of point defects, such as As antisites and As interstitials, and the epilayer is strained. The strain in the LT-GaAs is relaxed with post-growth anneals and this strain relaxation is accompanied by precipitation of the excess As.

Figure 3 shows a BF TEM cross-sectional image of of the as-grown LT-GaAs samples annealed at 600 °C for 10 min with MBE under an As atmosphere. As-grown LT-GaAs have highly non-stoichiometric structure with the excess arsenic in the form of point defects such as an arsenic anti-site (As_{Ga}), arsenic interstitial and gallium vacancy (V_{Ga}). Melloch *et al.* showed, with after growth annealing above 400 °C for 10 min, arsenic interstitial moving outside and precipitating to form arsenic precipitates. The As precipitates appear as dark circular spots, with diameters of 2 to 5 nm, and the shapes are spherical or ellipsodial as depicted in the inset of Fig. 3. With sufficient annealing above 600 °C for 10 min, As clusters are started to form from the bonding of As precipitate. The sizes of As clusters are increased as the annealing temperature increased. The As clusters appear as dark circular spots, with diameters more than 5 nm.[13)]

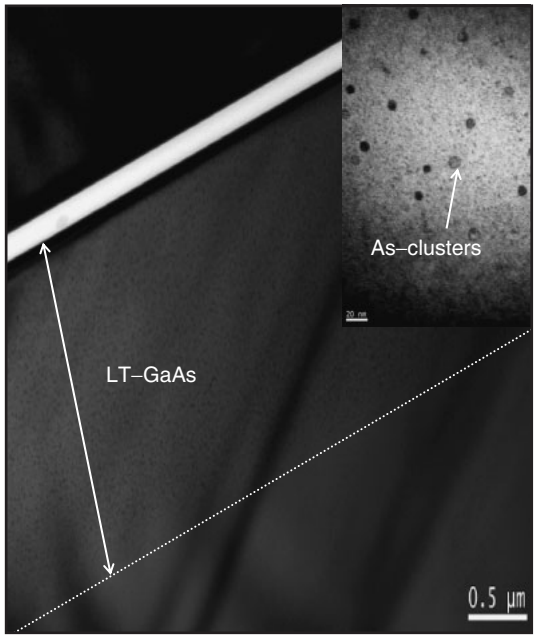

Fig. 3. Cross-sectional view of LT-GaAs samples annealed at 600 °C with MBE under an As atmosphere.

Moreover, there is almost no difference in contrast between the LT-GaAs and the GaAs substrate. The only distinction is the appearance of the As clusters that formed during the post-growth annealing.

Figure 4 shows HR-TEM images of samples from the LT-GaAs (sample A) for the following conditions: (a) an as-grown sample do not annealed; (b) an annealed sample at 400 °C for 10 min; and (c) an annealed sample at 600 °C for 10 min with MBE under an As atmosphere. The As cluster, which was not observed at an annealing temperature below 400 °C, started to form above 400 °C and could be seen clearly as the annealing temperature rose to 600 °C. We assume that at an annealing temperature above 400 °C, the

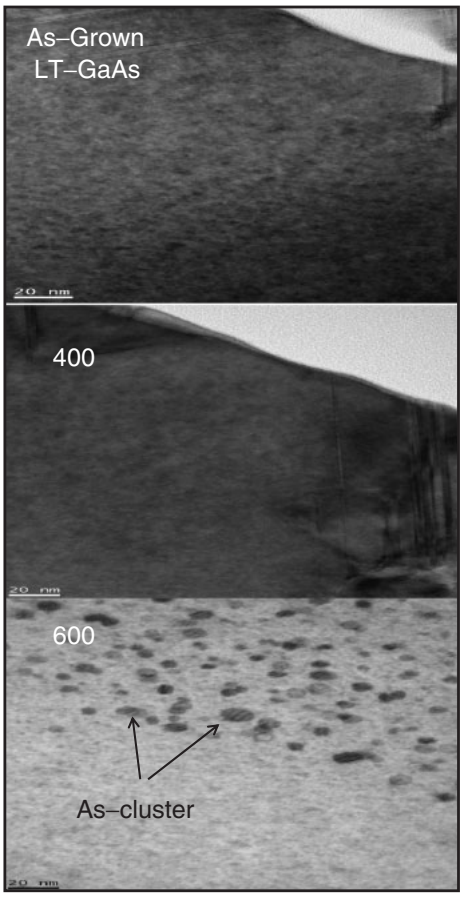

Fig. 4. Cross-sectional HR-TEM micrograph of LT-GaAs (sample A): (a) as-grown samples; (b) samples annealed at 400 °C; and (c) samples annealed at 600 °C with MBE under an As atmosphere.

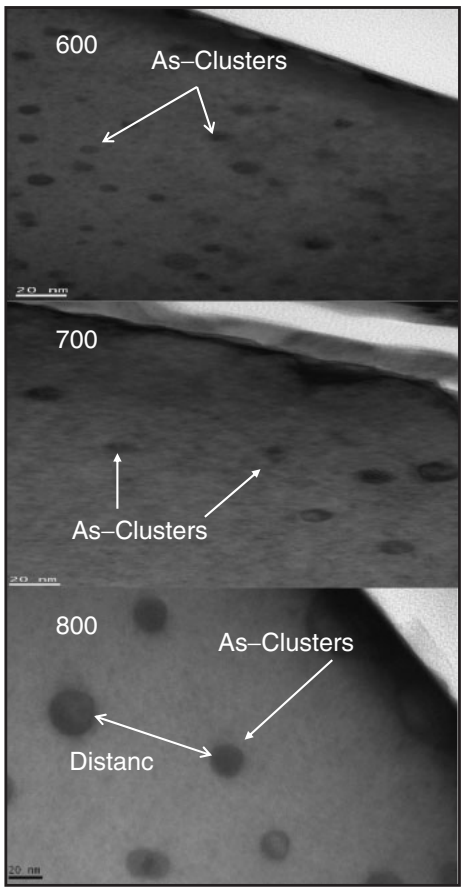

Fig. 5. Cross-sectional HR-TEM micrograph of LT-GaAs (sample B) annealed at (a) 600, (b) 700, and (c) 800 °C with RTA under an N_2 atmosphere.

excess As moves actively and is incorporated into the As precipitates; and that the As clusters begin to from as the annealing temperature rises between 400 and 600 °C.

Figure 5 shows HR-TEM images of the annealed LT-GaAs (sample B) at the following temperatures for 10 min: (a) annealed at 600 °C; (b) annealed at 700 °C; and (c) annealed at 800 °C with RTA in N_2 atmosphere. The density of As clusters decreases as the annealing temperature increases; furthermore, the sample annealed at 600 °C has a much higher density of As clusters than the samples annealed at 700 and 800 °C. The coarsening of As clusters is enhanced as the annealing temperature increases and, as shown in Fig. 5, the size of the As clusters increases. In addition, the distance between the As clusters increases as the annealing temperature increases. Therefore we assume that carrier lifetime increases as the annealing temperature increases due to the increase in the travel distance of the carriers. The coarsening of the As cluster occurs because the two-phase system of As clusters in the LT-GaAs matrix minimizes free energy with annealing by reducing the interfacial area between the As precipitates and the GaAs matrixes by means of the Ostwald ripening process.[14)]

Figure 6 shows the influence of the annealing process on the (004) reflex of LT-GaAs can be seen. The curves are calibrated to the (004) GaAs substrate reflex. Furthermore, the curves of the as-grown LT-GaAs show a double peak structure resulting from a difference in the lattice parameters of the substrate (higher angle) and the LT-GaAs epilayer

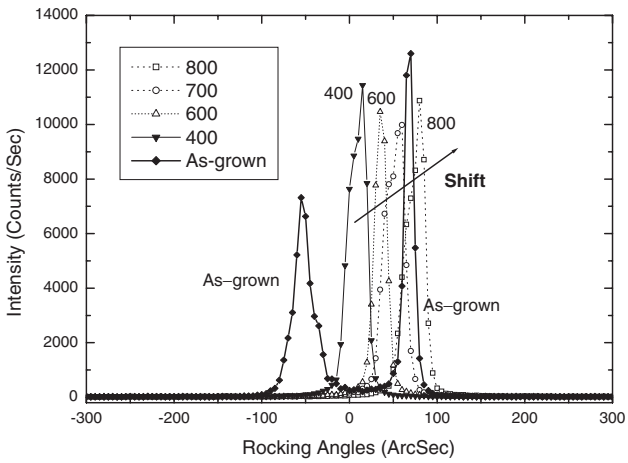

Fig. 6. X-ray diffraction rocking curves of an LT-GaAs wafer annealed at temperatures ranging from 400 to 600 °C under an As atmosphere and annealed above 700 °C with RTA under an N_2 atmosphere.

(lower angle). The difference in the lattice parameters is due to the lattice expansion that occurred when the excess As was incorporated as an As antisite, As interstitial and the gallium vacancy.

The electrooptical properties of LT-GaAs, such as the carrier trapping time (lifetime) and resistance, are governed by point defects generated by the incorporation of excess As. The double X-ray peak of the as-grown LT-GaAs becomes

Table I.

Annealing temperature (°C)	400	600
Resistivity ρ (Ω cm)	44509	90169
Hall coefficient R_H (m^3/C)	−26.64	−50.16
Bulk charge concentration n (cm^{-3})	2.346×10^{11}	1.246×10^{11}
Sheet charge concentration n_s (cm^{-2})	2.815×10^{7}	1.50×10^{7}
Mobility μ ($cm^2\,V^{-1}\,s^{-1}$)	599	556

to single peak with increasing the annealing temperature at 400 °C. Post-growth annealing results in a relaxation of the lattice expansion generated by incorporation of excess As and most of the recovery occurs with annealing at 400 °C. The recovery of the lattice constant is associated with decrease of point defects due to the movement of As interstitials and the formation of As clusters with increasing the annealing temperature. Therefore, the full width at half maximum (FWHM) decreases as the annealing temperature rises. The FWHM broadens again defects formation from the As evaporation as the annealing temperature rises above 800 °C. At a higher annealing temperature above 700 °C, the X-ray peak of the annealed LT-GaAs appears to the right of the substrate GaAs peak, indicates lattice contraction occurred by the out-diffusion of As. The peak position of the annealed LT-GaAs above 700 °C, shifts to higher angle as the annealing temperature increased from 600 to 800 °C.

Table I shows the resistivities of the post-growth annealed samples (sample A) as a function of the annealing temperature. In LT-GaAs much of the excess arsenic, with concentrations of 1–2%, can be in the form of the arsenic antisite (As_{Ga}), the arsenic interstitials (As_i), the gallium vacancy (V_{Ga}), and complex of these defects. The ionized As_{Ga}^{+} with concentrations of up to $(1–5) \times 10^{18}\,cm^{-3}$ in the LT-GaAs was observed and acted as donors. This concentration of As_{Ga}^{+} is equal to the concentration of ionized acceptors, presumably the ionized V_{Ga}^{-}. Because of the large concentration of point defects, the as-grown LT-GaAs exhibits hopping conduction with resistivities as low as 200 Ω cm and a mobility of $200\,cm^2\,V^{-1}\,s^{-1}$.[13]

With after growth annealing above 400 °C for 10 min, arsenic interstitial moving outside and precipitating to form arsenic precipitates. This negatively charged As precipitates attract the positively ionized atoms from surroundings and form the depletion region. Therefore, the resistivity increases if the distance between As clusters is close enough. Since the whole depletion region in the annealed LT-GaAs layer increases as the distance between As clusters become close. If the background doping is sufficiently low in relation to the spacing of As clusters, the LT-GaAs is completely depleted, and will exhibits a high resistivity more than 10^5 Ω cm.[13] Therefore, the resistance and mobility of the LT-GaAs samples annealed above 400 °C are significantly greater than the corresponding values of the as-grown values.[17]

We obtained terahertz spectra by using a 5-μm dipole antenna fabricated on the annealed LT-GaAs ranging from 600 to 700 °C. However, we did not observed terahertz spectra for the LT-GaAs samples annealed at 400 and 800 °C. Figure 7 shows the waveform of an electromagnetic wave pulses emitted from a 5-μm dipole on LT-GaAs for

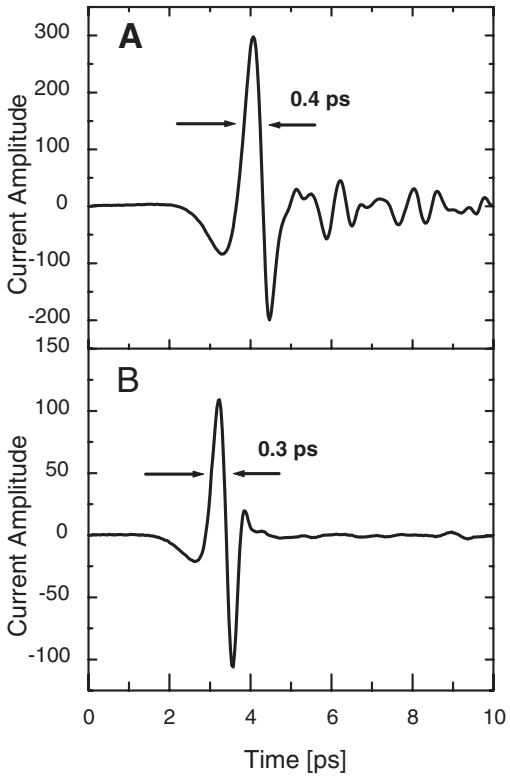

Fig. 7. Terahertz radiation pulse generated by dipole antenna I on LT-GaAs annealed at (a) 600 and (b) 700 °C.

the following annealing conditions: (a) an annealed sample at 600 °C with MBE under an As atmosphere; and (b) an annealed sample at 700 °C with RTA under an N_2 atmosphere. We applied a bias voltage of 10 V to the source electrode, and we used 20 mW for the pump and 8 mW for the probe beam. The widths of the main peak in Fig. 7 are 0.4 and 0.3 ps. Figure 8 shows the Fourier-transformed spectral amplitude detected by using a 5-μm dipole on silicon-on-sapphire (SOS) wafers. The spectral distributions are centered at 1.0 THz and the spectral widths are extended from 3.3 to 4.5 THz.

From the previous TEM analysis results, we conclude that the coarsening of As clusters is enhanced as the annealing temperature increases and the size of the As clusters increases. In addition, the distance between the As clusters increases as the annealing temperature increases. Therefore carrier lifetime increases as the annealing temperature increases due to the increase in the travel distance of the carriers. The GaAs samples which have the short lifetime less than 200 fs, reportedly do not show terahertz spectra due to the high absorption coefficients. For example, carrier lifetimes are 165 fs for p-type GaAs and 56 fs for n-type GaAs. And the absorption coefficients are $300\,cm^{-1}$ for p-type GaAs and $500\,cm^{-1}$ for n-type GaAs at 0.5 THz.[18] Also the carrier lifetime is known to increase from 300 fs to 1.64 ps as the annealing temperature rise from 500 to 800 °C.[19] We therefore did not obtain terahertz spectra for the samples annealed below 400 °C due to the large absorption (carrier trapping) by point defects. Also we did not observe terahertz spectra for the LT-GaAs samples annealed above 800 °C due to the point defects formation occurred by As evaporation. We only obtained terahertz

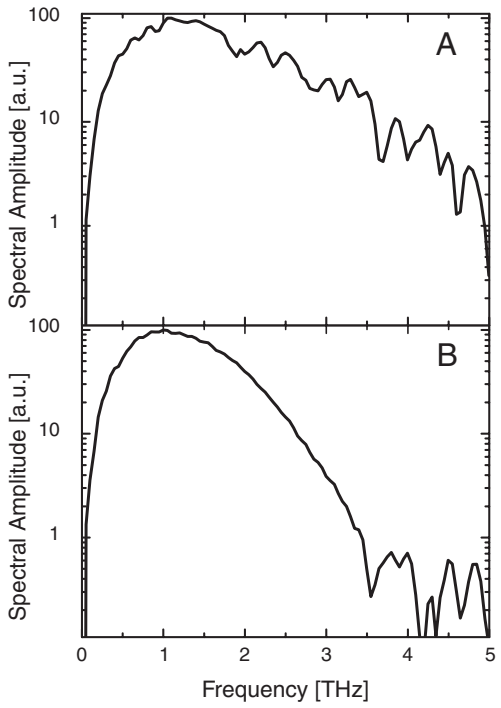

Fig. 8. Terahertz detection pulse detected by dipole antenna II on silicon-on-sapphire annealed at (a) 600 and (b) 700 °C.

spectra for the LT-GaAs samples annealed between 600 and 700 °C.

4. Conclusions

The annealing conditions were optimized for obtaining the terahertz emission and obtained terahertz spectra for the LT-GaAs samples annealed ranging from 600 to 700 °C but did not observe terahertz spectra for the LT-GaAs samples at the temperature range below 500 and above 800 °C.

The excess As that is incorporated into GaAs during low-temperature growth manifest itself in the form of point defects, such as As antisites and As interstitials, and the epilayer is strained. The strain in the LT-GaAs is relaxed with post-growth anneals and this strain relaxation is accompanied by precipitation of the excess As. The As clusters are not observable at annealing temperature below 400 °C but begins to form above 400 °C and can be seen clearly as the annealing temperature rises to 600 °C. As the annealing temperature increases, the density of the As clusters decreases and the distance of As cluster increases.

The double X-ray peak of the as-grown LT-GaAs becomes a single peak as the annealing temperature increases. Furthermore the FWHM decreases as the annealing temperature rises to 600 °C and broadens again as the annealing temperature rises to 800 °C. Post-growth annealing results in a strain relaxation and FWHM becomes a single peak for all annealing temperature above 400 °C. The recovery of strain is associated with the movement of As interstitials and forming As precipitates as the annealing temperature increases.

The resistivity and mobility of the LT-GaAs samples annealed in the range of 400 and 600 °C are significantly greater than the corresponding values of the as-grown samples. We selected a post-growth annealing at 600 °C as a best condition for obtaining the time domain of the terahertz radiation spectra. The width of the main peak of the pulse is 0.4 ps and its spectral distribution in the frequency domain extends to approximately 4.5 THz.

Acknowledgements

This work was supported by a grant from the Ministry of Information and Communication of Korea, under project no. A1100-0601-0110. The authors would like to thank Mr. Han-Chul Ryu, Mr. Seung-Byum Kang, Mr. Se-Young Jung, Min-Hwan Kwack, Mun-Chul Baek, and Mr. Seung-Hwan Lee of the Electronics and Telecommunications Research Institute (ETRI), for the device design and fabrication. They also thank to Dr. Chul Kang of the Advanced Photonic Research Institute for helpful discussions; Mr. Young-Bin Gee and Professor Tae-In Jeon of the Korea Marine University for terahertz measurements and analysis; Mrs. Jung-Suck Lee of the ETRI for X-ray measurements; Miss Soo-Hyun Kang and Mr. Kyooho Jung of the Dong-Guk University for Hall measurements; and Mr. Dae-Won Kang and Mr. Ju-Wook Lee of the ETRI for TEM Analysis.

1) F. W. Smith, A. R. Calawa, C. Chen, M. J. Manfra, and L. J. Mahoney: IEEE Electron Device Lett. **9** (1988) 77.
2) A. C. Warren, J. M. Woodall, J. L. Freeout, D. Grischkowsky, D. T. McInturff, M. R. Melloch, and N. Otsuka: Appl. Phys. Lett. **57** (1990) 1331.
3) J. N. Miller and T. S. Low: J. Cryst. Growth **111** (1991) 30.
4) X. Liu, A. Prasad, W. M. Chen, A. Kurpiewski, A. Stoschek, Z. Liliental-Weber, and E. R. Weber: Appl. Phys. Lett. **65** (1994) 3002.
5) D. C. Look: Thin Solid Films **231** (1993) 61.
6) U. Siegner, M. Haiml, F. Morier-Genoud, R. C. Lutz, P. Specht, E. R. Weber, and U. Keller: Physica B **273–274** (1999) 733.
7) H. S. Loka, S. D. Benjamin, and P. W. E. Smith: Opt. Commun. **161** (1999) 232.
8) M. Lagadas, K. Tsagaraki, Z. Hatzopoulos, and A. Christou: J. Cryst. Growth **127** (1993) 76.
9) R. Takahashi, Y. Kawamura, and H. Iwamura: Appl. Phys. Lett. **68** (1996) 153.
10) R. Mendis, C. Sydlo, J. Sigmund, M. Feiginov, P. Meissner, and H. L. Hartnagel: Solid-State Electron. **48** (2004) 2041.
11) W. Bartels: J. Vac. Sci. Technol. B **1** (1983) 338.
12) M. Hart: J. Phys. E **12** (1979) 911.
13) M. R. Melloch, J. M. Woodall, E. S. Harmon, N. Otsuka, F. H. Pollak, D. D. Nolte, R. M. Feenstra, and M. A. Lutz: Annu. Rev. Mater. Sci. **25** (1995) 547.
14) P. W. Voorhees: J. Stat. Phys. **38** (1985) 231.
15) M. H. Zhang, Y. F. Zhang, and J. M. Zhou: J. Cryst. Growth **209** (2000) 37.
16) P. W. Yu, D. N. Talwar, and C. E. Stutz: Appl. Phys. Lett. **62** (1993) 2608.
17) D. C. Look, D. C. Walters, M. O. Manasreh, J. R. Sizelove, C. E. Stutz, and K. R. Evans: Phys. Rev. B **42** (1990) 3578.
18) N. Katzenellenbogen and D. Grischkowsky: Appl. Phys. Lett. **61** (1992) 840.
19) I. S. Gregory and C. Baker: Appl. Phys. Lett. **83** (2003) 4199.